Subcycle Pulsed Focused Vector Beams

Qiang Lin,[1,2,*] Jian Zheng,[1] and Wilhelm Becker[2]
[1]*Institute of Optics, Department of Physics, Zhejiang University, Hangzhou 310027, China*
[2]*Max-Born-Institut, Max-Born-Strasse 2a, 12489 Berlin, Germany*
(Received 13 July 2006; published 19 December 2006)

An accurate description of a subcycle pulsed beam (SCPB) is presented based on the complex-source model. The fields are exact solutions of Maxwell's equations and applicable to a focused pulsed beam with a pulse duration down to and below one cycle of the carrier wave and with arbitrary polarization state. Depending on the pulse duration, the pulse is blueshifted, and its wings are chirped. This effect, which we refer to as ''self-induced blueshift'' goes beyond the carrier-envelope description. The corresponding phase is a temporal analog of the Gouy phase. The energy gain of a relativistic electron swept over by an SCPB is very sensitive to the proper form chosen to describe the pulse.

DOI: 10.1103/PhysRevLett.97.253902 PACS numbers: 42.65.Re, 31.15.−p, 41.75.Jv

The generation and application of intense few-cycle and single-cycle laser pulses is a rapidly increasing field of research; for reviews, see [1,2]. The theoretical description of ultrashort pulses and their linear and nonlinear propagation characteristics has caught the interest of many researchers. But, largely, the scalar approximation has been employed and the pulse has been represented as the product of a carrier wave and an envelope, assuming a pulse duration longer than about one cycle of the carrier wave [3]. Peak intensities of current few-cycle pulses are reaching into the relativistic regime [4,5]. Therefore, more than ever, an accurate description of the pulse-matter interaction requires precise knowledge of all components of the electromagnetic field.

In this Letter, we will present analytical expressions of few-cycle, single-cycle, and subcycle pulsed beams (SCPBs) with arbitrary polarization that are exact solutions of Maxwell's equations. The solutions are generated with the help of the complex-source method [6–8]. They contain the scalar pulsed Gaussian beam as a special case if the paraxial approximation is adopted. We discuss the spatiotemporal structure of the solutions and compare with the scalar approximation. We find that for a subcycle pulsed beam the instantaneous frequency is highest at the center of the pulse and always higher than the frequency of the carrier wave—an effect that is suppressed by the carrier-envelope description. We will call this a ''self-induced blueshift'' since it is enforced by Maxwell's equations *in vacuo* and does not require any specific pulse-matter interaction. The consequences of this effect are illustrated by the example of electron acceleration by an SCPB in the relativistic regime.

Consider two opposite charges oscillating against each other. We may describe them by an oscillating dipole located at the origin of the coordinate system with the dipole moment

$$\mathbf{p}(\mathbf{r}, t) = \frac{p_0(t)}{\sqrt{1+\xi^2}}(\mathbf{e}_x + i\xi\mathbf{e}_y)\delta(\mathbf{r}), \tag{1}$$

where the parameter ξ determines the polarization state, such that $\xi = 0$ corresponds to linear polarization in the x direction, $\xi = \pm 1$ to circular polarization, and $\xi = \pm\infty$ to linear polarization in the y direction. The function $p_0(t)$ is, in principle, arbitrary. Here we model it by the product of a carrier wave with frequency $\omega = kc = 2\pi/T_0$ (c is the speed of light *in vacuo*) and a positive-definite envelope, for which we take a Gaussian with a FWHM of $2\sqrt{2\ln 2}T$,

$$p_0(t) = p_0 \exp\left(-\frac{t^2}{2T^2}\right)\exp(i\omega t + i\phi_0). \tag{2}$$

The peak value p_0 of the dipole moment determines the peak power of the beam, as will be shown below, and ϕ_0 denotes the carrier-envelope phase or absolute phase. Our results will be specific for this product form, but not to the Gaussian shape of the envelope.

The oscillating dipole (1) emits a spherically outgoing electromagnetic pulse. A focused pulse propagating in a certain direction, for which we take the z direction, can be obtained by moving the source dipole from the origin to a complex position along the z axis. This is a very useful mathematical technique to obtain focused propagating solutions of Maxwell's equations. According to this complex-source-point model [6–8], we introduce the spatiotemporal translation

$$z \to z' = z + iz_0, \qquad t \to t' = t - t_0 + i\frac{z_0}{c}. \tag{3}$$

We shift both the spatial coordinate z and the time ct by the same imaginary amount. This way, on axis (for $x = y = 0$) the shift cancels from the retarded time, and we will be able to retrieve the standard Gaussian beam in the paraxial approximation. In the latter, the parameter $z_0 = kw_0^2/2$ will become the Rayleigh range determined by the beam waist w_0. We introduce the complex distance

$$R' = \sqrt{x^2 + y^2 + (z + iz_0)^2}, \tag{4}$$

which is a double-valued function. We have to choose the proper branch to ensure that the solution is a "beam," i.e., that it does not diverge in the transverse dimension [7].

We obtain the fields by folding the source with the infinite-space Green function [9]:

$$\mathbf{E}\,(x,y,z,t) = \frac{c^2\mu_0 k^2 p_0(\tau')}{4\pi R'\sqrt{1+\xi^2}}\left[f(\mathbf{e}_x + i\xi\mathbf{e}_y) + \frac{x+i\xi y}{R'^2} g\mathbf{r}\right], \tag{5}$$

$$\mathbf{H}(x,y,z,t) = \frac{ck^2 h p_0(\tau')}{4\pi R'^2\sqrt{1+\xi^2}}[-i\xi z'\mathbf{e}_x + z'\mathbf{e}_y + (i\xi x - y)\mathbf{e}_z], \tag{6}$$

where μ_0 is the magnetic permeability of the vacuum, and the source $p_0(\tau')$ as well as the functions

$$f = \left(1 + \frac{i\tau'}{\omega T^2}\right)^2 - \frac{1}{k^2R'^2}\left(1 - \frac{t'R'}{cT^2} + ikR'\right),$$
$$g = -f + \frac{2}{k^2R'^2}\left(1 - \frac{\tau'R'}{cT^2} + ikR'\right), \qquad h = f + \frac{1}{k^2R'^2}. \tag{7}$$

are evaluated at the complex retarded time $\tau' = t' - R'/c$.

The physical fields are obtained as the real parts of the fields (5) and (6). Inserting the fields into Maxwell's equations allows one to identify the generating current in real space. The peak value E_0 of the electromagnetic field is related to the (time-dependent) Poynting vector $\mathbf{S} = \mathrm{Re}(\mathbf{E}) \times \mathrm{Re}(\mathbf{H})$ of the beam through $E_0 = \sqrt{c\mu_0 S_{\max}}$. This yields the relation $p_0 = 4\pi z_0 A_0 E_0/(c^2k^2\mu_0)$, where $A_0^{-2} = [B + 1/(k^2z_0^2)]B$ with $B = 1 - 1/(kz_0) + 1/(\omega^2T^2)$. The components of the electric and magnetic field of the SCPB now are

$$E_x = \mathrm{Re}\left[A\left(f + \frac{x\bar{x}g}{R'^2}\right)\right], \qquad B_x = \mathrm{Re}\left[-A\frac{i\xi z'}{R'c}h\right],$$
$$E_y = \mathrm{Re}\left[A\left(i\xi f + \frac{\bar{x}yg}{R'^2}\right)\right], \qquad B_y = \mathrm{Re}\left[A\frac{z'}{R'c}h\right], \tag{8}$$
$$E_z = \mathrm{Re}\left[A\frac{\bar{x}z'}{R'^2}g\right], \qquad B_z = \mathrm{Re}\left[A\frac{i\xi x - y}{R'c}h\right],$$

where $\bar{x} = x + i\xi y$, $A = E_0z_0A_0p_0(\tau')/(p_0R'\sqrt{1+\xi^2})$.

Panels (a)–(c) of Fig. 1 show the three components of the electric field for linear polarization in the x direction [$\xi = 0$ in Eq. (1)], while panel (d) exhibits the E_z component for circular polarization ($\xi = 1$). We see that the transverse component E_x of the SCPB has a Gaussian profile in the transverse dimension x, with its maximum on the propagation axis ($x = 0$). In contrast, the transverse component E_y and the longitudinal component E_z are zero along this axis and assume their (much smaller) extrema around $|x| \approx w_0$. Even though the electric source dipole (1) is linearly polarized in the x direction [for panels (a)–(c)], the transverse component E_y of the SCPB is not equal to zero. However, its peak value is reduced by more than 1 order of magnitude compared with the x component.

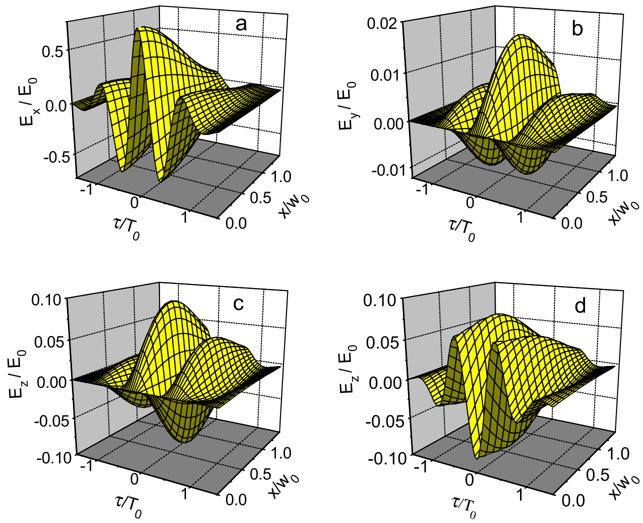

FIG. 1 (color online). Profiles of the electric-field components for $\lambda = 2\pi c/\omega = 1.054\ \mu$m, $T = 0.5T_0$, $w_0 = 1\ \mu$m, $\phi_0 = 0.5\pi$, $t_0 = 0$ at $y = 0.5w_0$ and $z = 0$ as functions of τ and x for linear polarization (a)–(c) and circular polarization (d) of the generating dipole (1). Note the different scales for the various field components.

Therefore, the strongly focused beam is no longer strictly linearly polarized. Moreover, the transverse focusing has enforced a nonzero longitudinal component. The temporal profiles of E_x, E_y, and E_z are all different. Panel (d) shows that for circular polarization the longitudinal component E_z is nonzero along the propagation axis.

In order to elucidate the structure of the general SCPB (8) for $\xi = 0$, we will first consider the limit of a plane wave. The expressions can be obtained by letting the beam waist $w_0 \to \infty$ in Eq. (8). For $\xi = 0$, we obtain

$$E_x = \mathrm{Re}\{-iE_0[p_0(\tau)/p_0]A_d(0)^{-1}A_d(\tau)\}, \tag{9}$$

where

$$A_d(\tau) = \left(1 + \frac{i\tau}{\omega T^2}\right)^2 + \frac{1}{\omega^2T^2}, \tag{10}$$

and $B_y = E_x/c$, while all other field components vanish. The field depends on position only via the retarded time $\tau = t - t_0 - z/c$ so that its wave fronts (surfaces of constant phase) are planes. Owing to the complex factor $A_d(\tau)$, the field (9), unlike the source (2), is no longer the product of a carrier wave and an envelope. Its total phase is

$$\phi(\tau) = \omega\tau + 2\arctan[\mathrm{sgn}(\tau)\sqrt{1+\alpha^2} - \alpha] + \phi_0 - \pi/2, \tag{11}$$

with $\alpha = (1 + \omega^2T^2 - \tau^2/T^2)/(2\omega\tau)$. The corresponding instantaneous frequency $\omega_e(\tau) = d\phi(\tau)/d\tau$ satisfies

$$\omega_e(0) \geq \omega_e(\tau) > \omega. \tag{12}$$

Hence, the τ-dependent frequency is highest at the center of the pulse and blueshifted with respect to the carrier-wave frequency ω throughout the entire pulse [10]. Moreover, the pulse is chirped on either side of $\tau = 0$. These effects are strong when T is small compared with T_0, in which case the center frequency can significantly exceed the carrier frequency. We will refer to the frequency shift as a self-induced blueshift (SIBS).

Figure 2 shows the temporal profiles of plane-wave subcycle pulses for different pulse durations with and without the SIBS taken into account. The latter case is realized by replacing the factor $A_d(0)^{-1}A_d(\tau)$ in Eq. (9) by unity. It is evident that in the subcycle region, the SIBS greatly affects the temporal profile. For $T > T_0$, on the other hand, its effect quickly disappears. Figure 2(d) shows the integral of the electric-field component E_x over time for the plane-wave pulse when the factor $A_d(\tau)/A_d(0)$ in Eq. (9) is replaced by unity. The presence of the SIBS causes this integral to be zero, as can easily be seen analytically. If the SIBS is dropped, for $T \ll T_0$ the integral acquires a substantial nonzero value, revealing the presence of a large dc component. Under quite general assumptions [11], a laser field will satisfy the condition $\int E(\mathbf{r}, t)dt = 0$ at fixed position $\mathbf{r}$. A field that violates this condition may cause artifacts, which will be illustrated by the example below.

In order to see the relation of the general SCPB to the standard pulsed Gaussian beam [12,13], as a second special case we investigate the paraxial limit where the transverse coordinates are small compared with the longitudinal coordinate z. To this end, we expand R' to second order in x and y:

$$R' = z + iz_0 + \frac{1}{2}\frac{\rho^2}{z + iz_0} + \cdots, \tag{13}$$

where $\rho^2 = x^2 + y^2$. The x component of the linearly

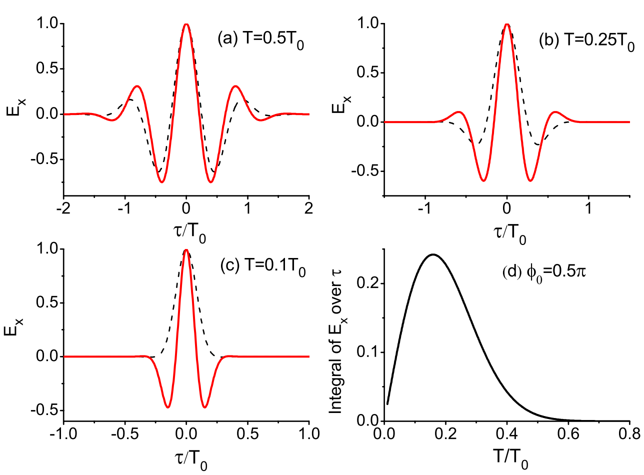

FIG. 2 (color online). Temporal profiles of the x component of a linearly polarized cosine-type pulse ($\phi_0 = \frac{\pi}{2}$, $z = 0$) in the plane-wave limit ($w_0 \to \infty$) for different pulse durations with (solid line) and without (dashed lines) the self-induced blueshift [panels (a)–(c)]. Panel (d) shows the time integral of E_x in the latter case.

polarized pulse (8) then becomes

$$E_x = \mathrm{Re}[E_0 A_p(\tau, z)A_{c-e}(\tau, z, \rho)A_{s-t}(\tau, z, \rho)B^{-1}], \tag{14}$$

where

$$A_p(\tau, z) = A_d(\tau) - \frac{i}{k(z + iz_0)}\left(1 + \frac{i\tau}{\omega T^2}\right), \tag{15}$$

$$A_{c-e}(\tau, z, \rho) = \frac{z_0}{z + iz_0}\frac{p_0(\tau)}{p_0}\exp\left(-\frac{ik}{2}\frac{\rho^2}{\rho(z)} - \frac{\rho^2}{w(z)^2}\right), \tag{16}$$

$$A_{s-t}(\tau, z, \rho) = \exp\left[\left(1 - i\frac{z_0}{z}\right)\frac{\tau}{2cT^2}\frac{\rho^2}{\rho(z)}\right], \tag{17}$$

with $\rho(z) = z + z_0^2/z$ the radius of curvature of the wave front and $w(z) = (w_0/z_0)\sqrt{z^2 + z_0^2}$ the beam width. We have dropped terms of order R'^{-2} and higher. To the same order, E_y and B_x vanish and E_z and B_z are of the order of z^{-1}. The function $A_{c-e}(\tau, \rho, z)$ contains the source function (2) and the standard Gaussian exponential. This is multiplied by the function $A_{s-t}(\tau, \rho, z)$, which goes to unity in the limit of large T, but mixes the dependence on τ, z, and ρ in a characteristic fashion if T is comparable with or smaller than the carrier-wave period T_0. The total phase of the pulse (14),

$$\Phi(\rho, z, \tau) = \bar{\phi}(\tau) + \psi(z, \rho) - \frac{z_0}{z}\frac{\tau}{2cT^2}\frac{\rho^2}{\rho(z)}, \tag{18}$$

is the sum of the phase $\bar{\phi}(\tau) = \omega\tau + \arg(A_p(\tau, z)) + \phi_0 - \pi/2$ [note that $\arg(A_p(\tau, z))$ generalizes the phase $\phi(\tau)$ of Eq. (11)], the phase

$$\psi(z, \rho) = \arctan[2z/(kw_0^2)] - k\rho^2/[2\rho(z)] \tag{19}$$

of a stationary Gaussian pulse, and a spatiotemporal coupling phase, which is a characteristic novel feature of the SCPB.

The total phase (18) contains both the common Gouy phase [the first term on the right-hand side of Eq. (19)] and the SIBS phase [the second term on the right-hand side of Eq. (11)]. The latter is caused by the finite pulse duration, while the Gouy phase is due to the finite lateral spatial extent of the pulse [14,15]. The SIBS phase exists for any pulse of finite duration just as the Gouy phase exists for any focused pulse. However, only when the pulse duration approaches the single-cycle regime, will the SIBS phase become noticeable.

Next we address physical manifestations of the SIBS. Let us calculate the acceleration of a free electron by the SCPB (8) by solving numerically the relativistic equations of motion for an electron in a laser field [16–19], $d\mathbf{r}_e/dt = \frac{\mathbf{p}_e}{\gamma}$ and $d\mathbf{p}_e/dt = -\mathrm{Re}\mathbf{E} - \frac{\mathbf{p}_e}{\gamma c} \times \mathrm{Re}\mathbf{B}$, where $\mathbf{r}_e$ and $\mathbf{p}_e$ are the position and the mechanical momentum of the electron, and $\gamma = \sqrt{1 + \mathbf{p}_e^2/c^2}$ in atomic units. We let the electron

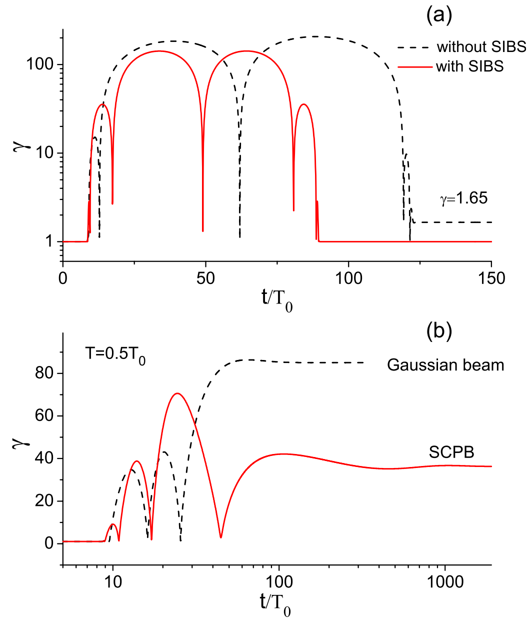

FIG. 3 (color online). The relativistic factor $\gamma \equiv E/(mc^2)$ of a free electron accelerated by the SCPB (8) with peak intensity $I = 1 \times 10^{21}$ W/cm^2 and $T = 0.5T_0$ under various approximations: (a) Limit of a plane wave ($w_0 \rightarrow \infty$) with [solid (red) line] and without [dashed (black) line] SIBS; (b) exact sine ($\phi_0 = 0$) SCPB as given by Eq. (8) with $w_0 = 2$ μm compared with a Gaussian pulse obtained by neglecting the SIBS.

start from the position $\mathbf{r}_0 = (0, 0, 0)$ with zero velocity at an early time ($t = -10T_0$) before the arrival of the SCPB.

Panel (a) of Fig. 3 shows the electron energy as a function of time for the cosine ($\phi_0 = \pi/2$) plane-wave SCPB (9). If the SIBS is ignored as described above so that the pulse acquires a nonzero dc component, the electron leaves the pulse with a substantial final energy, corresponding to $\gamma = 1.65$. This violates the known fact that the net acceleration of a free electron by a plane-wave field is zero [20]. As we have shown, an SCPB being a solution of Maxwell's equations automatically includes the SIBS. If this is properly taken into account, according to Eq. (9), the curve $\gamma(t)$ is exactly symmetric about the pulse's central peak, and the net energy gain becomes zero, as it should. Figure 3(b) compares the electron acceleration by a focused subcycle Gaussian sine beam as given by Eq. (8) and by a standard Gaussian sine beam in the paraxial and the carrier-envelope approximation. The standard Gaussian sine beam is described by Eq. (14) with $A_p(\tau, z) = 1$ and $B = 1$. Again, there are substantial differences between the energy gain due to the exact pulse and the approximated Gaussian pulse. The latter exaggerates the net energy gain by a factor of more than 2 ($\gamma = 84$ rather than $\gamma = 35$ for the exact pulse). Note that the energy gain of an electron that is swept over by a focused pulse is not necessarily zero, unlike in the case of a plane-wave pulse discussed above.

In conclusion, we have presented exact analytical expressions for the electric and magnetic fields of focused subcycle pulsed beams. Their precise form is critically important in the calculation of the physical effects caused by subcycle pulses. The crucial feature is the existence of a temporal analog of the Gouy phase. This phase introduces a frequency blueshift of the pulse, which is maximal at its center. In the relativistic regime, this blueshift has a significant effect on the energy gain of an electron that is swept over by the pulse. If it is neglected, the gain may come out much too large.

We thank A. Fedotov and S. P. Goreslavski for a critical reading of the manuscript. Q. L. gratefully acknowledges support from the Alexander von Humboldt Foundation. This work was supported in part by the NSFC of China (Grants No. 10574110 and No. 10334050).

*Electronic address: qlin@zju.edu.cn

[1] T. Brabec and F. Krausz, Rev. Mod. Phys. **72**, 545 (2000).
[2] Y. I. Salamin, S. X. Hu, K. Z. Hatsagortsyan, and C. H. Keitel, Phys. Rep. **427**, 41 (2006).
[3] T. Brabec and F. Krausz, Phys. Rev. Lett. **78**, 3282 (1997).
[4] A. J. Verhoef, J. Seres, K. Schmid, Y. Nomura, G. Tempea, L. Veisz, and F. Krausz, Appl. Phys. B **82**, 513 (2006).
[5] T. Fuji, N. Ishii, C. Y. Teisset, X. Gu, Th. Metzger, A. Baltuška, N. Forget, D. Kaplan, A. Galvanauskas, and F. Krausz, Opt. Lett. **31**, 1103 (2006).
[6] G. A. Deschamps, Electron. Lett. **7**, 684 (1971).
[7] E. Heyman and L. B. Felsen, J. Opt. Soc. Am. A **6**, 806 (1989).
[8] Z. Wang, Q. Lin, and Z. Wang, Phys. Rev. E **67**, 016503 (2003).
[9] J. D. Jackson, *Classical Electrodynamics* (Wiley, New York, 1999), 3rd ed.
[10] Actually, Eq. (12) holds for an arbitrary pulse with vector potential $\mathbf{A}(\tau) = \mathbf{e}\Psi(\tau)\cos(\omega\tau + \phi_0)$ and scalar potential $\Phi = 0$ for reasonable envelopes $\Psi(\tau)$, at least if τ is sufficiently close to the central maximum of the envelope, between the turning points on either side of the maximum. It can be shown that $\omega_e(\tau)/\omega = 1 + (\Psi'^2 - \Psi\Psi'')/(\Psi'^2 + \omega^2\Psi^2)$, where $\Psi' = d\Psi/d\tau$.
[11] See, e.g., D. B. Milošević, G. G. Paulus, D. Bauer, and W. Becker, J. Phys. B **39**, R203 (2006).
[12] Z. Wang, Z. Zhang, Z. Xu, and Q. Lin, IEEE J. Quantum Electron. **33**, 566 (1997).
[13] E. Heyman and L. B. Felsen, J. Opt. Soc. Am. A **18**, 1588 (2001).
[14] S. Feng and H. G. Winful, Opt. Lett. **26**, 485 (2001).
[15] F. Lindner, G. G. Paulus, H. Walther, A. Baltuška, E. Goulielmakis, M. Lezius, and F. Krausz, Phys. Rev. Lett. **92**, 113001 (2004).
[16] N. B. Narozhny and M. S. Fofanov, JETP **90**, 753 (2000).
[17] S. X. Hu and A. F. Starace, Phys. Rev. Lett. **88**, 245003 (2002).
[18] A. Maltsev and T. Ditmire, Phys. Rev. Lett. **90**, 053002 (2003).
[19] Q. Lin, S. Li, and W. Becker, Opt. Lett. **31**, 2163 (2006).
[20] T. W. B. Kibble, Phys. Rev. A **150**, 1060 (1966).